

RFI SPATIAL PROCESSING AT NANÇAY OBSERVATORY : APPROACHES AND EXPERIMENTS

G. Hellbourg^{,**}, R. Weber^{*}, K. Abed-Meraim^{*}, A.J. Boonstra^{***}*

^{*}Laboratoire PRISME, Université d'Orléans, 45067 Orléans, France

^{**}Observatoire de Paris, Station de radioastronomie de Nançay, 18330 Nançay, France

^{***}ASTRON, P.O. Box 2, 7990 AA Dwingeloo, Netherlands

ABSTRACT

Because of the denser active use of the spectrum, and because of higher radio telescope sensitivities, radio frequency interference (RFI) mitigation has become a sensitive topic for current and future radio telescope designs. In this paper, we consider different interference mitigation options which take advantage of both time-frequency and spatial RFI signatures. After specific subspace decompositions, these RFI spatial signatures are estimated and applied to pre- or post-correlation data by means of spatial filtering techniques based on projectors. We provide some performance analysis through simulations and Cramer-Rao Lower Bound derivations. In addition, recent results on real data from the LOFAR and EMBRACE radio telescopes are presented.

Index Terms— RFI mitigation, Radio astronomy, Antenna array, Spatial filtering, Cyclostationarity

1. INTRODUCTION

The sensitivity of state-of-the-art radio telescopes is over ten orders of magnitude higher than in most communications systems. Although radio telescopes are best located in relatively remote areas, astronomical observations may still be hampered by man-made radio frequency interference (RFI). An exhaustive survey on RFI mitigation techniques for radio astronomy [1] and a recent workshop [2] dedicated to that topic have shown various developments for preserving quality of radio astronomical observations. Note however that, in routine practice, the majority of RFI mitigation procedures are based on corrupted data detection and flagging. For example, the operational Low Frequency Array (LOFAR) [3, 4], see figure 5, provides a post-correlation RFI classification tool based on combinatorial thresholding [5].

However, next generation radio telescopes such as the just mentioned LOFAR or the future Square Kilometre Array (SKA) [6] currently in an engineering phase, can offer much more options. Indeed, their multi-stage architecture (i.e. the telescope is an array of phased stations and each station is a phased antenna array) can lead, amongst others, to interesting RFI spatial filtering approaches. This paper addresses

interference spatial processing at the station stage, i.e. before central correlation [7].

Consider an arbitrary array of M antennas. The N_c cosmic sources and N_r RFI sources are assumed to be uncorrelated. They are also assumed to be uncorrelated to the system noise. Assuming the narrow band hypothesis holds, the data covariance matrix is given by [8] ($(\cdot)^H$ refers to the hermitian transpose):

$$\mathbf{R} = \underbrace{\mathbf{A}_r \mathbf{R}_r \mathbf{A}_r^H}_{\mathbf{R}_{\text{RFI}}} + \underbrace{\mathbf{A}_c \mathbf{R}_c \mathbf{A}_c^H}_{\mathbf{R}_{\text{cosmic}}} + \mathbf{R}_{\text{noise}} \quad (1)$$

- $\mathbf{A}_r = [\mathbf{a}_{r_1} \dots \mathbf{a}_{r_{N_r}}]$ the $(M \times N_r)$ interference spatial signature matrix, where each column vector \mathbf{a}_{r_k} is the spatial signature of the k^{th} interference,
- $\mathbf{A}_c = [\mathbf{a}_{c_1} \dots \mathbf{a}_{c_{N_c}}]$ the $(M \times N_c)$ cosmic source spatial signature matrix,
- \mathbf{R}_c (resp. \mathbf{R}_r), the cosmic source (resp. the RFI) diagonal power matrix,
- $\mathbf{R}_{\text{noise}}$ the $(M \times M)$ system noise correlation matrix taking in account the sky and electronic noise contributions, including potential coupling.

It is assumed that cosmic source contributions are buried in the noise (or negligible) and that the system noise is calibrated with equal power σ_n^2 on each antenna after applying a whitening step [9, 10] (i.e. $\mathbf{R}_{\text{noise}} = \sigma_n^2 \mathbf{I}$). In [8, 11, 12] spatial filtering techniques are proposed, based on the RFI spatial signature estimation, \mathbf{A}_r , followed by a subspace projection to remove that dimension from \mathbf{R} .

In Section 2 the approach based on eq. (1) is extended to include cyclostationary properties of the RFI signals. As a benchmark, we present the Cramer Rao Lower Bound (CRLB) for some specific statistical Gaussian models. In Section 3, several spatial filtering techniques are described. Finally, Section 4 presents some experimental results with observed radio telescope data.

2. RFI SUBSPACE ESTIMATION

In order to mitigate the interference contributions through spatial filtering, we need to estimate a set of vectors spanning the subspace determined by \mathbf{A}_r .

With the simplified model mentioned in the previous section (i.e. $\mathbf{R} = \mathbf{A}_r \mathbf{R}_r \mathbf{A}_r^H + \sigma_n^2 \mathbf{I}$), a singular value decomposition (SVD) leads to the expected result. Indeed, in this case, the RFI subspace is spanned by the Singular Vectors (SV) associated to the N_r dominant singular values of \mathbf{R} .

When cosmic sources contributions are no longer negligible, or when the noise is not calibrated [10], the RFI subspace estimation must be based on other properties, as presented hereafter.

2.1. Cyclostationary and time-lag approaches

Most telecommunication signals show cyclostationary properties due to periodic characteristics of their modulation schemes [13]. By modifying the radio telescope correlator input data, a cyclic correlation matrix, $\mathbf{R}^{\alpha, \tau}$, can be computed:

$$\mathbf{R}^{\alpha, \tau} = E \{ \mathbf{y}_\alpha(t - \tau/2) \mathbf{y}_{-\alpha}(t + \tau/2)^H \} \quad (2)$$

where $\mathbf{y}_\alpha(t) = \mathbf{x}(t)e^{-j\pi\alpha t}$, $E \{ \cdot \}$ is the expected value (in case of observed data, the expected value is replaced by $\langle \cdot \rangle_N$, the time averaging operator over N samples), and α and τ are related hidden periodicities of the (interfering) telecommunication signals. Assuming a cyclostationary RFI signal impinges on the antenna array, and assuming cosmic sources and system noise signals are stationary by nature over a short time scale, we have

$$\mathbf{R}^{\alpha, \tau} = \mathbf{R}_{\text{RFI}}^{\alpha, \tau} + \underbrace{\mathbf{R}_{\text{cosmic}}^{\alpha, \tau}}_{\rightarrow \mathbf{0}} + \underbrace{\mathbf{R}_{\text{noise}}^{\alpha, \tau}}_{\rightarrow \mathbf{0}} = \mathbf{A}_r \mathbf{R}_r^{\alpha, \tau} \mathbf{A}_r^H \quad (3)$$

with $\mathbf{R}_r^{\alpha, \tau}$ containing cyclic information. Applying an SVD to $\mathbf{R}^{\alpha, \tau}$ leads to RFI subspace estimation, that is the set of SV corresponding to the non-zero (principal) singular values of $\mathbf{R}^{\alpha, \tau}$. A similar approach can be followed using the cyclic conjugated correlation matrix [14].

Assuming that cosmic sources and system noise are almost white in the considered band, we can simplify eq (2) by limiting α to 0. Thus, for non-white telecommunication signals, if we can find a set of time-lags $\tau_0 > 0$ for which $\mathbf{R}_{\text{cosmic}}^{0, \tau_0}$ and $\mathbf{R}_{\text{noise}}^{0, \tau_0}$ are equal to zero while $\mathbf{R}_{\text{RFI}}^{0, \tau_0}$ is not, then the RFI subspace can be estimated using the cyclostationary approach described in [15].

The different RFI subspace estimation techniques presented are based on an SVD of one particular type of covariance matrix. Since in practise a covariance matrix is calculated over a finite number of samples, the use of several matrices could increase the estimation accuracy. In [15] the RFI subspace is evaluated by joint diagonalization of multiple cyclic and time-lagged covariance matrices.

For all these methods, more details and results with simulated data are given in [15, 16]. In this paper however, experimental results are given, in the last section. Before presenting performance simulations, we will present the CRLB for some Gaussian signals cases.

2.2. Gaussian CRLB

Here we consider the case of one RFI source signal in additive white Gaussian noise [17]:

$$\mathbf{x}(t) = \mathbf{a}_r r(t) + \mathbf{n}(t) \quad (4)$$

where $r(t)$ is either Gaussian stationary iid with zero mean and power σ_r^2 (Gaussian Model: GM), or $r(t) = e^{j(\omega t + \psi)} s(t)$ where $\omega/2\pi$ is an unknown carrier frequency, ψ an unknown phase parameter and $s(t)$ a zero mean iid real Gaussian signal of power σ_r^2 (cyclostationary Modulated Gaussian Model: MGM). The antenna array is assumed to have uncalibrated phases (but calibrated magnitudes [9, 10]), and hence the steering vector takes the general form $\mathbf{a}_r = [1, e^{j\phi_1}, \dots, e^{j\phi_{M-1}}]^T$ where $\phi_1, \dots, \phi_{M-1}$ are unknown phase parameters. The parameter vector containing the unknowns corresponds to

$\Theta = [\phi_1, \dots, \phi_{M-1}, \sigma_r^2, \sigma_n^2]^t$ for the Gaussian model and to $\Theta = [\phi_1, \dots, \phi_{M-1}, \sigma_r^2, \sigma_n^2, \omega, \psi]^t$ for the modulated Gaussian model. We refer to $\Phi = [\phi_1, \dots, \phi_{M-1}]^t$ as the set of desired parameters (the others are the nuisance parameters). The CRLB w.r.t. the desired parameter vector Φ is derived using the procedure described in [9] (details are omitted due to space limitation).

$$CRLB(\phi_k)_{k=1, \dots, M-1} = \frac{(1 + \text{Minr})}{M \text{inr}^2 N} \quad (\text{GM}) \quad (5)$$

$$CRLB(\phi_k)_{k=1, \dots, M-1} = \frac{(1 + 2\text{Minr})}{2M \text{inr}^2 N} \quad (\text{MGM}) \quad (6)$$

where the Interference-to-Noise Ratio (inr) is σ_r^2/σ_n^2 and N is the number of samples. In the MGM case, N is a multiple of the period $2\pi/\omega$ in order to neglect the edge effects.

Similar results on the direction of arrival have been obtained in [18]. In particular, both results show that using cyclostationary properties improve estimation performance at low inr by a factor 2.

From the previous equations, we can derive the CRLB for the spatial signature vector \mathbf{a}_r and we can define the lower bound for the dot product between true and estimated signature vector:

$$E \left\{ \left\| \frac{\mathbf{a}_r^H \hat{\mathbf{a}}_r}{M} - 1 \right\|^2 \right\} \geq \frac{M-1}{2M} CRLB(\phi_k) \quad (7)$$

where $\hat{\mathbf{a}}_r$ is the estimated spatial signature.

Figure 1 shows a comparison between the different interference subspace estimation techniques presented here.

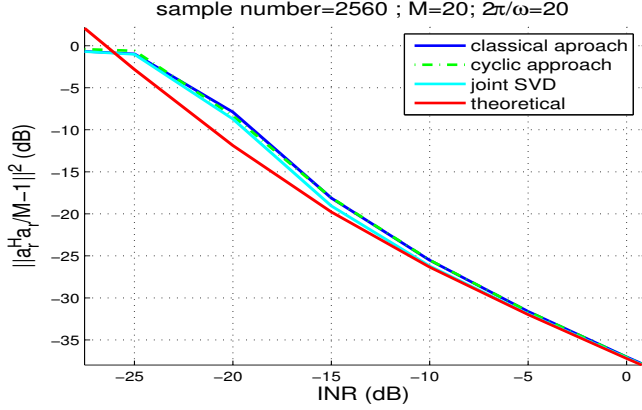


Fig. 1. Comparison of three different interference subspace estimation techniques and their CRLB on the MGM data model according to the inr.

The performance of the techniques are quantified according to the criterion defined in eq. (7), averaged over 1000 trials. The simulated interference is based on the MGM case, with $M = 20$ antennas, $2\pi/\omega = 20$ and $N = 2560$ samples. RFI subspaces are estimated through an SVD where the dominant SV is used as an estimation of \mathbf{a}_r .

The joint SVD approach consists in joint diagonalizing a cyclic and a classic covariance matrix using an extended SVD [15].

At low inr (inr < -15 dB), the estimated performance diverges from the theoretical estimate. This effect is due to the restricted range of the parameters involved in the simulation (e.g. $\phi_k \in [-\pi, +\pi]$).

The joint SVD approach has lower variance than any other estimator. At high inr, the performances of all the estimators converge toward the CRLB.

3. SPATIAL FILTERING BY PROJECTION TECHNIQUES

Once the interference subspace has been estimated, spatial filters can be built and applied at the antenna array output. Although exhaustive beamforming techniques can be found in the literature [19, 20], the techniques presented here are limited to projection approaches. These approaches consist of reducing the radio telescope data vector space dimension by removing the interference subspace contributions.

The orthogonal projector nulling the interference subspace \mathbf{A}_r for example is defined as [21]:

$$\mathbf{P}_{\mathbf{A}_r}^\perp = \mathbf{I} - \mathbf{A}_r (\mathbf{A}_r^H \mathbf{A}_r)^{-1} \mathbf{A}_r^H \quad (8)$$

This projector can either be applied at the antenna array output (at the pre-correlation stage) or on the data correlation

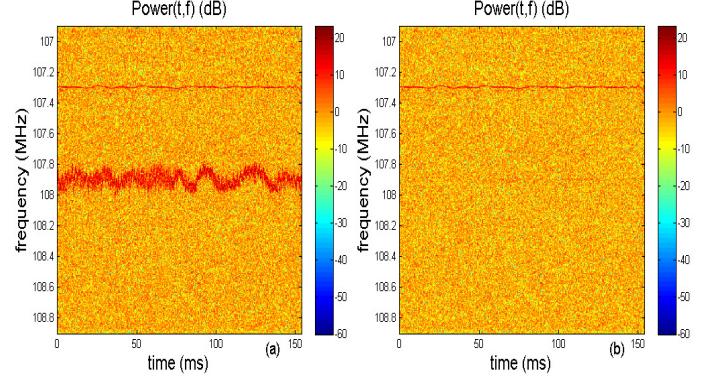


Fig. 2. (a) LOFAR observation in the FM frequency band. (b) LOFAR observation after orthogonal projection of the strongest FM interference.

matrix (at the post-correlation stage) leading to:

$$\mathbf{x}_{clean}(t) = \mathbf{P}_{\mathbf{A}_r}^\perp \mathbf{x}(t) = \mathbf{P}_{\mathbf{A}_r}^\perp (\mathbf{A}_c \mathbf{c}(t) + \mathbf{n}(t)) \quad (9)$$

$$\mathbf{R}_{clean} = \mathbf{P}_{\mathbf{A}_r}^\perp (\mathbf{A}_c \mathbf{R}_c \mathbf{A}_c^H + \mathbf{R}_{noise}) \mathbf{P}_{\mathbf{A}_r}^{\perp H} \quad (10)$$

To preserve the power of the source of interest, oblique projection has been proposed in [16]. With \mathbf{A}_r the interference subspace and \mathbf{w} the steering vector corresponding to the direction of interest, the oblique projection is defined as [16]:

$$\mathbf{E}_{\mathbf{w}\mathbf{A}_r} = \mathbf{w} (\mathbf{w}^H \mathbf{P}_{\mathbf{A}_r}^\perp \mathbf{w})^{-1} \mathbf{w}^H \mathbf{P}_{\mathbf{A}_r}^\perp \quad (11)$$

Suppose the cosmic source $c_k(t)$, with steering vector \mathbf{a}_{ck} , is of interest, we replace in eq. (9) $\mathbf{P}_{\mathbf{A}_r}^\perp$ by $\mathbf{E}_{\mathbf{w}\mathbf{A}_r}$.

4. REAL DATA PROCESSING

Some results of RFI mitigation processing applied on real radio telescope data are presented here, as well as an oblique projection based algorithm implementation.

4.1. LOFAR data

Figure 2.(a) shows the Time Frequency representation of an observation made with the radio interferometer LOFAR[3, 4]. This observation is corrupted by two strong Frequency Modulated (FM) signals.

An orthogonal projection method has been applied to this observation. The interference subspace was estimated using the classic covariance matrix of the observation. One single SV has been selected to estimate the strongest RFI subspace. Figure 2.(b) shows a time-frequency representation of the same observation after applying the orthogonal projection which clearly illustrates the effect of spatial RFI mitigation.

Figure 3 shows another example of orthogonal projection applied to LOFAR data. Figure 3.(a) is an all-sky (hemisphere) map, constructed by applying beamforming to the observed correlation matrix (in all directions in the sky), with

three cosmic sources and one interference at the horizon. Figure 3.(b) is a skymap created with a 1-sample time-lag covariance matrix. The cosmic sources are no longer visible. Figure 3.(c) corresponds to the corrected skymap, once the interference has been projected out.

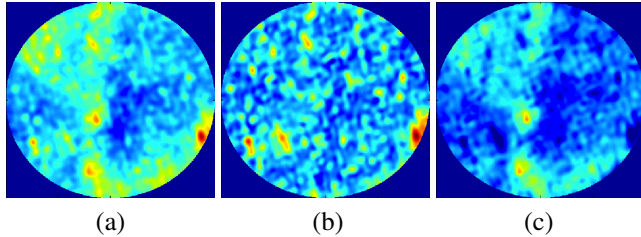


Fig. 3. (a) LOFAR skymap with cosmic sources in the centre and interference on the horizon. (b) Skymap based on a 1-sample time lag covariance matrix, only interference is visible. (c) LOFAR skymap after orthogonal projection.

4.2. EMBRACE data

An RFI mitigation algorithm has been implemented at the French station of the demonstrator EMBRACE [22] (see Fig. 5). EMBRACE is a dense aperture array that provides a one second covariance matrix (*crosslet*) and a beamformed signal (*beamlet*) corresponding to a frequency of interest. The crosslet is used to estimate the interference subspace dimension through a Minimum Description Length (MDL) approach [23], and a subspace basis is estimated with a classical SVD.

Once the interference subspace has been estimated, an oblique projector is built, taking into account the interference subspace as well as a direction of interest. The resulting projection matrix is finally applied to the antenna array to provide a clean beamlet.

EMBRACE can also scan a wider frequency band. In this case, a crosslet corresponding to one single subband is provided each second and the full frequency bandwidth is scanned in 512 seconds. After 512 seconds, the scan restarts at the first frequency subband of the frequency bandwidth of interest. Real time RFI mitigation can not be achieved in this mode since the corrections would only be applied every 512 seconds, after the interference subspace has been estimated. The data can however be corrected offline.

Figure 4 shows an observation made in this mode. The green graph is a non-corrected signal corresponding to a GPS drift scan. Some other interference can be seen on this observation, particularly a strong home-made narrow band interference at the middle of the frequency bandwidth. The blue graph is the same observation corrected with an orthogonal projection, and the red graph is the observation corrected by an oblique projection. As we can see, the oblique projection better recovers an interference-free observation.

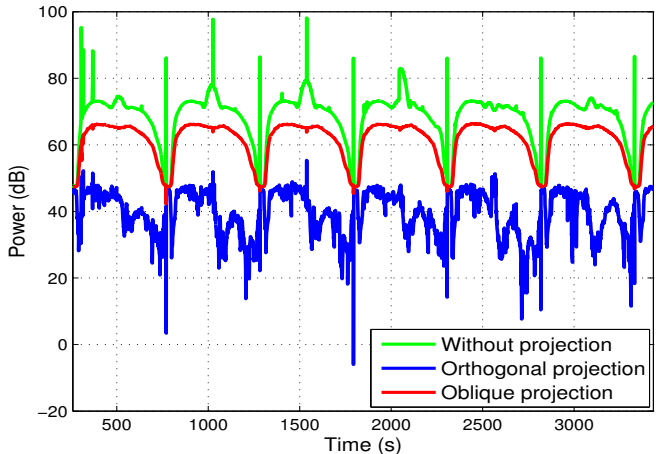


Fig. 4. GPS satellite drift scan and other interference recorded with EMBRACE working in the full bandwidth mode. Blue and red graphs correspond to the same observation, respectively corrected by an orthogonal and an oblique projection.



Fig. 5. Nançay observatory showing a French LOFAR station (left), and the French EMBRACE station (right).

5. CONCLUSION

In this article we presented different spatial filtering strategies for interference mitigation using phased antenna arrays in radio astronomy. The spatial diversity, as well as RFI characteristics, provide information allowing better RFI subspace estimation, and therefore mitigation, than classical projection methods.

These results however should not be misinterpreted to imply possible ways to soften radio regulation agreements. Indeed, mitigation always includes cost both in terms of investments and often also in terms of signal integrity. In practice, RFI mitigation counter measures should be balanced in the sense that the cost of including RFI measures in the design is justified in terms of regained spectrum.

6. REFERENCES

- [1] A.J. Boonstra and R. Weber, “RFI mitigation method inventory,” Tech. Rep., SKA Design Study report, 2009.

- [2] “RFI 2010 conference, Groningen, The Netherlands,” Proceedings of Science (PoS), March 29-31 2010.
- [3] M. de Vos, “LOFAR: the first of a new generation of radio telescopes,” in *Acoustics, Speech, and Signal Processing, 2005. Proceedings. (ICASSP '05). IEEE International Conference on*, 2005, vol. 5, pp. v/865–v/868 Vol. 5.
- [4] van Haarlem, M. P. et al., “LOFAR: The LOW-Frequency ARray,” *Astronomy and Astrophysics*, vol. 556, pp. A2, Aug. 2013.
- [5] A. R Offringa, A. G de Bruyn, M. Biehl, S. Zaroubi, G. Bernardi, and V. N Pandey, “Postcorrelation radio frequency interference classification methods,” *Monthly Notices of the Royal Astronomical Society*, vol. 405, no. 1, pp. 155–167, June 2010.
- [6] SKA web site., “<http://www.skatelescope.org>,”.
- [7] A. Leshem and A.-J van der Veen, “Radio-astronomical imaging in the presence of strong radio interference,” *Information Theory, IEEE Transactions on*, vol. 46, no. 5, pp. 1730–1747, 2000.
- [8] A. Leshem, A.J. van der Veen, and A.J. Boonstra, “Multichannel Interference Mitigation Techniques in Radio Astronomy,” *The Astrophysical Journal Supplement Series*, vol. 131, no. 1, pp. 355–373, November 2000.
- [9] A.-J. Boonstra and A.-J. van der Veen, “Gain calibration methods for radio telescope arrays,” *Signal Processing, IEEE Transactions on*, vol. 51, no. 1, pp. 25–38, Jan 2003.
- [10] Amir Leshem and A.-J van der Veen, “Multichannel detection of Gaussian signals with uncalibrated receivers,” *Signal Processing Letters, IEEE*, vol. 8, no. 4, pp. 120–122, 2001.
- [11] J. Raza, A.J. Boonstra, and A.J. van der Veen, “Spatial Filtering of RF Interference in Radio Astronomy,” *IEEE Signal Processing Letters*, vol. 9, no. 2, pp. 64–67, February 2002.
- [12] S. van Der Tol and A.-J. van der Veen, “Performance analysis of spatial filtering of RF interference in radio astronomy,” *Signal Processing, IEEE Transactions on*, vol. 53, no. 3, pp. 896–910, 2005.
- [13] William A Gardner, *Statistical spectral analysis: a non-probabilistic theory*, Prentice-Hall, Inc., 1986.
- [14] Grégory Hellbourg, Rodolphe Weber, Cécile Capdessus, and Albert-Jan Boonstra, “Cyclostationary approaches for spatial RFI mitigation in radio astronomy,” *Comptes Rendus Physique*, vol. 13, no. 1, pp. 71 – 79, 2012, The next generation radiotelescopes / Les radiotélescopes du futur.
- [15] G. Hellbourg, T. Trainini, R. Weber, E. Moreau, C. Capdessus, and A.J. Boonstra, “RFI subspace estimation techniques for new generation radio telescopes,” in *Signal Processing Conference (EUSIPCO), 2012 Proceedings of the 20th European*, 2012, pp. 200–204.
- [16] G. Hellbourg, R. Weber, C. Capdessus, and A.-J. Boonstra, “Oblique projection beamforming for RFI mitigation in radio astronomy,” in *Statistical Signal Processing Workshop (SSP), 2012 IEEE*, 2012, pp. 93–96.
- [17] A. Leshem and A.-J. van der Veen, “Multichannel detection and spatial signature estimation with uncalibrated receivers,” in *Statistical Signal Processing, 2001. Proceedings of the 11th IEEE Signal Processing Workshop on*, 2001, pp. 190–193.
- [18] S.V. Schell and W.A. Gardner, “The Cramer-Rao lower bound for directions of arrival of Gaussian cyclostationary signals,” *Information Theory, IEEE Transactions on*, vol. 38, no. 4, pp. 1418–1422, 1992.
- [19] Barry D Van Veen and Kevin M Buckley, “Beamforming: A versatile approach to spatial filtering,” *ASSP Magazine, IEEE*, vol. 5, no. 2, pp. 4–24, 1988.
- [20] Vijay Madisetti, *Wireless, networking, radar, sensor array processing, and nonlinear signal processing*, CRC Press, 2010.
- [21] A.-J. Boonstra, *Radio frequency interference mitigation in radio astronomy*, Ph.D. thesis, Technische Universiteit Delft (The Netherlands), 2005.
- [22] G.W. Kant, P.D. Patel, S.J. Wijnholds, M. Ruiter, and E. Van der Wal, “EMBRACE: A Multi-Beam 20,000-Element Radio Astronomical Phased Array Antenna Demonstrator,” *Antennas and Propagation, IEEE Transactions on*, vol. 59, no. 6, pp. 1990–2003, 2011.
- [23] Tülay Adali and Simon Haykin, *Adaptive signal processing: next generation solutions*, vol. 55, Wiley. com, 2010.